

Published in final edited form as:

Nat Immunol. 2014 November ; 15(11): 1017–1025. doi:10.1038/ni.2987.

Neutrophils sense microbial size and selectively release neutrophil extracellular traps in response to large pathogens

Nora Branzk¹, Aleksandra Lubojemska¹, Sarah E. Hardison², Qian Wang¹, Maximiliano G. Gutierrez³, Gordon D. Brown², and Venizelos Papayannopoulos^{1,*}

¹Division of Molecular Immunology, Medical Research Council National Institute for Medical Research, Mill Hill, London, UK

²Aberdeen Fungal Group, University of Aberdeen, Institute of Medical Sciences, Foresterhill, Aberdeen, United Kingdom

³Division of Mycobacterial Research, Medical Research Council National Institute for Medical Research, Mill Hill, London, UK.

Abstract

Neutrophils are critical for antifungal defense, but the mechanisms that clear hyphae and other pathogens that are too large to be phagocytosed remain unknown. We show that neutrophils sense microbial size and selectively release neutrophil extracellular traps (NETs) in response to large pathogens, such as *Candida albicans* hyphae and extracellular *Mycobacterium bovis* aggregates, but not small yeast and single bacteria. NETs are fundamental in countering large pathogens *in vivo*. Phagocytosis via dectin-1, acts as a sensor for microbial size preventing NETosis by downregulating neutrophil elastase (NE) translocation to the nucleus. Dectin-1 deficiency leads to aberrant NETosis and NET-mediated tissue damage during infection. Size-tailored neutrophil responses clear large microbes and minimize pathology when microbes are small enough to be phagocytosed.

INTRODUCTION

The immune system controls microbes of varying size ranging from small viruses and bacteria, to dimorphic fungi and large multicellular parasites. Large microbes and parasites evade phagocytosis and can prove difficult to clear^{1, 2}. It is unknown how the immune system senses microbial size and clears large pathogens. There has been significant progress in our understanding of how immune receptors distinguish between soluble and particle-associated microbial ligands³. However, little is known about how immune cells distinguish between microbial particles of varying size and whether they can differentially respond to combat microbes of varying size.

Users may view, print, copy, and download text and data-mine the content in such documents, for the purposes of academic research, subject always to the full Conditions of use:http://www.nature.com/authors/editorial_policies/license.html#terms

*Correspondence to: vpapaya@nimr.mrc.ac.uk.

AUTHOR CONTRIBUTIONS: NB performed all experiments except from mouse infections with *A. fumigatus* that were performed by SEH and GEB and immunoblotting and neutrophil immunofluorescence microscopy performed by NB, OL, QW and VP. MGG advised and contributed in the *M. bovis* BCG experiments. VP devised and directed the study. NB and VP wrote the manuscript.

Fungi present a significant challenge to the immune system as they grow in a small yeast form that can be countered by phagocytosis and a filamentous form that is too large to be phagocytosed. Both small and large forms are thought to be critical for fungal virulence. Due to its large size, the filamentous form is resilient to the immune system while the small yeast or spores are required for dissemination⁴. Macrophages release higher concentrations of the cytokine interleukin-1 β in response to hyphae than in response to yeast⁵, but the mechanism driving this differential response and most importantly, the significance of this hypersensitivity for fungal clearance are unclear.

Neutrophils are critical in controlling fungal infections that cause potentially lethal infections in neutropenic and immunosuppressed individuals^{6, 7}. While neutrophils kill yeast by phagocytosis and release factors that indirectly starve the fungus of important metal ions⁸, how neutrophils directly kill filamentous hyphae is poorly understood. Neutrophils were long thought to undertake a single antimicrobial program involving phagocytosis and degranulation^{9, 10}. The discovery of neutrophil extracellular traps (NETs)¹¹ raised the question as to whether neutrophils can deploy their antimicrobial strategies selectively, to generate an efficient immune response that is tailored to pathogens with different attributes.

NETs are large, extracellular, web-like structures composed of decondensed chromatin and neutrophil antimicrobial factors. NETs trap and kill a variety of microbes¹⁰ but their contribution to innate immune defense is unclear. NETs are released primarily via a cell death program that requires reactive oxygen species (ROS), and the granule proteins myeloperoxidase (MPO) and neutrophil elastase (NE)^{12, 13}. Upon activation, NE is released from azurophilic granules into the cytosol and translocates to the nucleus where it cleaves histones to decondense chromatin¹⁴. Myeloperoxidase consumes H₂O₂ to generate HOCl and other oxidants and is required for NE translocation to the nucleus during NETosis and chromatin decondensation^{14, 15}. Fungi trigger NETosis and are killed by NETs¹². Furthermore, NET-deficiency is associated with fungal susceptibility in chronic granulomatous disease patients who do not generate ROS¹⁶ and in MPO-deficient patients^{17, 18}. A human case study hinted that NETs may play a critical antifungal role by controlling the large filamentous form¹⁶, but due to the requirement of ROS and MPO in phagocytic killing, the importance of NETs in antifungal immunity has been difficult to dissect.

The aberrant release and defective clearance of NETs has also been associated with various human pathologies such as autoimmune systemic lupus erythematosus (SLE) and ANCA vasculitis. Although, their interplay is poorly understood, fungal infection and aberrant NETosis are implicated in inflammatory and autoimmune disease^{19, 20}. Therefore, NETosis must be tightly regulated but the mechanisms that control their deployment in different scenarios remain unknown.

Here, we identify a cell-autonomous mechanism that allows immune cells such as neutrophils to sense microbial size. We show that by regulating the size-dependent release of NETs, this mechanism allows for the selective implementation of neutrophil antimicrobial strategies to clear fungal infections while minimizing tissue damage.

RESULTS

NETosis depends on microbial size

To address how neutrophils respond to microbes of varying size, we tested several microbes for their capacity to induce NETosis in isolated human peripheral neutrophils. Fungal pathogens are good inducers of NETosis. Interestingly, NETosis required plasma in response to *Candida albicans* (Fig. 1a). Because plasma drives hyphal formation in *C. albicans* (Fig. 1a, phase, right panels), we investigated whether fungal morphology plays a role in NET formation. Strikingly, large preformed hyphae grown in RPMI medium induced NETosis in the absence of plasma (Fig. 1b and Supplementary Fig. 1a). In contrast, a yeast-locked *hgc1* mutant of *C. albicans*²¹, which cannot form hyphae, failed to induce NETosis in the presence of plasma or RPMI (Fig. 1b and Supplementary Fig. 1b). Finally, hyphae, but not yeast, triggered histone degradation in neutrophils (Fig. 1c), a key step in driving chromatin decondensation during NETosis¹⁴. These data suggest that NET release is selective and dependent on fungal morphology.

Aside from their difference in size, *C. albicans* yeast and hyphae also vary in metabolic activity and surface molecule expression^{22, 23}. Interestingly, selective NETosis was not dependent on microbial enzymatic activity, since heat-inactivated hyphae induced NET release as efficiently as live hyphae (Supplementary Fig. 1c, d). We tested whether selective NETosis was driven by expression of different fungal surface molecules or solely by a difference in microbial size, by presenting small yeast particles to neutrophils over a modified transwell that allowed for direct contact with the microbes but prevented phagocytosis. The transwell chamber rim was removed to enable the transwell to sink to the bottom of the well and bring neutrophils in contact with the membrane. The membrane pore size was small enough to prevent neutrophil transmigration and phagocytosis but large enough to allow neutrophils to extend filopodia and contact the microbes on the other side. To ensure that neutrophils were coming in contact with the microbes, we removed the modified transwell chamber after 1 h of incubation, rinsed the bottom, and imaged the cells with the membrane permeable DAPI DNA stain (Supplementary Fig. 1e). We found great neutrophil attachment to the bottom of the modified transwell chambers. In the presence of the transwell, small yeast particles triggered NETosis only when the transwell chamber was in direct contact with neutrophils (Fig. 1d, e) but not when the chamber sat higher in the well to prevent direct contact between neutrophils and microbes (Supplementary Fig. 1f). Hence, neutrophils were in physical contact with yeast in the modified transwell otherwise neutrophils in the suspended transwell would also yield NETs. Therefore, yeast only trigger NETosis when they are presented as larger particles. In contrast, heat-inactivated hyphae that were fragmented into particles small enough to be phagocytosed (Supplementary Fig. 2) lost their ability to induce NETosis (Fig. 1f, g). Therefore, selective NETosis is independent of fungal surface molecule expression or enzymatic activity and is regulated only by differences in microbial size. Consistently, neutrophils released NETs in response to *Aspergillus fumigatus* hyphae or large aggregated *A. fumigatus* conidia, but failed to form NETs in response to small single conidia (Supplementary Fig. 3).

Although bacteria are reported to induce NET release^{11, 13, 24, 25}, our data suggests that bacteria that are small enough to be phagocytosed would not induce NETosis. Consistently, neutrophils did not release NETs in response to *Escherichia coli* and *Klebsiella pneumoniae* (Fig. 2a, b), but induced NETosis, when presented through the transwell system (Fig. 2a, b). Many pathogenic bacteria are known to circumvent phagocytosis through virulence strategies that include the formation of large aggregates²⁶⁻²⁸. Clumping of *Mycobacterium* species is thought to prevent phagocytosis and contribute to pathogenesis²⁹. We incubated neutrophils with a mix of single bacteria, small and large aggregates of *M. bovis* BCG-dsRed (BCG-dsRed) and found that after 4 h, some neutrophils released NETs (Fig. 2c, d, group i) whereas others underwent necrosis with small nuclei that did not decondense (Fig. 2c, d, group ii). In these endpoint experiments, NETs seemed to be released by neutrophils that were associated with large bacterial aggregates. However, the accumulation of small phagocytosed bacteria in neutrophils makes it difficult to determine the original size of the bacterial particles that triggered these responses. Therefore, we observed neutrophils infected with BCG-dsRed by time-lapse video microscopy (Fig. 2e). While single bacteria were phagocytosed without triggering NETosis (Fig. 2e, asterisk), neutrophils failed to phagocytose large BCG-dsRed aggregates and eventually released NETs (Fig. 2e, arrowhead). Therefore, the size-dependence of NET release applies to fungi, bacteria and perhaps other large pathogens.

NETs control hyphae *in vivo*

Our findings suggested that perhaps NETs evolved as a specific mechanism to counter large hyphae extracellularly, as they cannot be phagocytosed. To address this important point we first examined whether NETs are released selectively *in vivo*. Interestingly, only WT *C. albicans* that can form both yeast and hyphae induced NET release in the lungs of WT mice (Fig. 3a). In contrast, the yeast-locked *hgc1* mutant, failed to induce NETosis indicating that neutrophils selectively release NETs in response to *C. albicans* size *in vitro* and *in vivo*. To address whether selective NETosis is critical to control the hyphal form, we infected MPO deficient mice that do not form NETs and WT controls, with a low dose of WT or yeast-locked *C. albicans*. WT mice that are able to both phagocytose and form NETs cleared both WT and yeast-locked *C. albicans* strains and fully recovered from the infection (Fig. 3b). Interestingly, MPO deficient mice that can only kill via phagocytosis cleared the *hgc1* yeast-locked strain that does not form hyphae, indicating that NETs were not required for clearance of yeast. In contrast, MPO deficient mice succumbed to infection with the WT fungus that forms both yeast and hyphae (Fig. 3b) indicating that while MPO-deficient mice could control yeast in the absence of NETs, they could not control hyphae. WT fungus established an infection in the lung of MPO-deficient animals and disseminated to the spleen (Fig. 3c). Therefore, NETs were required specifically to control the hyphal form. To exclude that these differences were due to the *hgc1* mutant being a non-pathogenic, attenuated strain that is slow to replicate and establish an infection *in vivo*, we infected NADPH oxidase-deficient mice where both phagocytic killing and NETosis are incapacitated. The yeast-locked *hgc1* mutant was comparably virulent with WT *C. albicans* in NADPH oxidase-deficient mice, suggesting that the mutant strain could establish an infection when neutrophil function was more severely abrogated (Supplementary Fig. 4). Together, our data

indicate that NETs are a critical strategy to control filamentous fungi that are too large to be cleared by phagocytosis.

Phagocytosis inhibits NETosis by sequestering NE

To investigate the mechanism that regulates size-dependent NETosis, we first examined the activation of Syk and ERK, two kinases involved downstream of fungal recognition and implicated in the NETosis pathway by triggering ROS production^{30, 31}. We found only subtle differences in the dynamics of phosphorylation of Syk upon induction with yeast or hyphae (Supplementary Fig. 5a). ERK appeared to be more strongly induced by hyphae. To examine if these differences in kinase activation were triggering differential ROS activation, we compared the neutrophil ROS burst in response to yeast and hyphae. We found two major classes of neutrophils in the population of healthy human donors. In half our donors ($n=6$) there was no major difference in ROS dynamics, while in the other half neutrophils exhibited a delayed response to yeast, but yielded much stronger ROS concentrations (Supplementary Fig 5b). Importantly, NETs were selectively released only in response to hyphae irrespectively of these variations in ROS dynamics among different human donors, indicating that while signaling via these kinases that regulate the ROS burst may be required for NETosis, it does not regulate the decision of whether to make NETs in response to microbial size.

We reasoned that size-dependent decision-making may be regulated downstream of ROS. Because phagocytosis proceeds faster than NETosis^{13, 32}, we hypothesized that the uptake of yeast could potentially sequester NE to the phagosome, preventing NE translocation to the nucleus. Hence, we monitored the localization of NE after stimulation with yeast or hyphae. We stained neutrophils for NE, MPO and DNA. NE and MPO colocalize in the same azurophilic granules in resting neutrophils, but NE selectively translocates to the nucleus during NET formation, leaving MPO behind¹⁴. We used the colocalization of NE with MPO and DNA to monitor NE translocation. In neutrophils stimulated with hyphae, NE translocated to the nucleus (Fig. 4a) with over 70% of the total NE in the nucleus 3 h post stimulation (Fig. 4b). In contrast, in neutrophils stimulated with yeast, less than 20% of the total NE was found in the nucleus (Fig. 4a, b) and was predominately co-localizing with MPO away from the nucleus. To investigate the fate of NE in yeast-treated neutrophils we stained for NE in combination with p40 and p47, two components of the NADPH oxidase that assemble on the phagosome membrane³², the azurophilic granule membrane marker CD63 and an antibody against the *C. albicans* cell wall. After stimulation with *C. albicans* yeast, NE and CD63 strongly co-localized with p40 and p47 around phagocytosed yeast (Fig. 4c-e), indicating that NE was being predominately recruited to the phagosome via fusion of azurophilic granules with the phagosome membrane – a well-characterized process^{32, 33}.

These results suggest that the fusion of the phagosome with azurophilic granules containing NE is the critical step in the regulation of selective NETosis. To test whether the sequestration of NE to the phagosome suppresses NET release in response to yeast, we blocked granule fusion with the phagosome by inhibiting acidification with bafilomycin A1 or microtubule polymerization with nocodazole. Both treatments increased NET formation

in response to *C. albicans hgc1* yeast (Fig. 5a) pointing to a simple competition mechanism where phagocytosis inhibits NETosis. Since ROS are important upstream effectors in NETosis we also examined whether these compounds elicited NETosis by increasing ROS levels. In contrast, bafilomycin A1 and nocadozole reduced ROS, as the assembly of the NADPH oxidase involves microtubule-enhanced fusion of specific granules with the phagosome membrane. Importantly, the remaining ROS concentrations were sufficient to trigger NETosis in response to yeast (Fig. 5b). Furthermore, pre-incubation of neutrophils with yeast to induce phagocytosis prior to induction of NETosis with hyphae, decreased the efficiency of NET release after re-stimulation with hyphae in a dose-dependent manner (Fig. 5c) highlighting the significance of NE availability to drive NET formation. NETosis was similarly inhibited by feeding neutrophils with opsonized polystyrene beads of similar size to yeast showing that the phagosome formation is sufficient to downregulate NETosis without a requirement for additional stimulation by microbial factors in yeast (Fig. 5d). Therefore, phagocytosis negatively regulates NETosis by depleting NE before it is able to translocate to the nucleus. This mechanism prevents unnecessary NET release when the pathogen is small enough to be eliminated intracellularly by phagocytosis and may help to fine-tune the immune response.

Dectin-1 negatively regulates NETosis

Next we tested whether the regulation of NETosis by phagocytosis is important in fine-tuning the immune response to reduce immune pathology. We reasoned that a deficiency in phagocytic receptor activity may disrupt the size-dependent selectivity of NET release due to inefficient phagocytosis. Dectin-1 is one of the major anti-fungal phagocytic receptors^{34, 35} and human primary neutrophils treated with a dectin-1 blocking antibody exhibited significantly reduced phagocytosis compared to untreated control neutrophils (Fig. 6a). Blocking dectin-1 reduced the rate of phagocytosis and neutrophils took up less than half the number of yeast. This residual phagocytosis is likely to be driven by other phagocytic receptors that quickly become saturated in the absence of active dectin-1. The reduction in phagocytosis correlated with a striking induction of NET release in response to *hgc1* yeast-locked *C. albicans* (Fig. 6b). In line with previous reports³⁶, in the absence of the blocking antibody, phagocytosing human neutrophils died after engulfing microbes to their maximum capacity, but failed to decondense their nuclei (Fig. 6c and Supplementary Movie 1) consistent with a lack of NE translocation to the nucleus (Fig 4a, b). In contrast, when phagocytosis was reduced in the presence of the anti-dectin-1 antibody, neutrophils readily decondensed their nuclei and made NETs in response to yeast (Fig. 6c and Supplementary Movie 2). Immunofluorescence microscopy showed that the amount of NE localized to the phagosome (Fig. 6d, arrows) in anti-dectin-1 treated neutrophils incubated with yeast for 1 h, was comparable to untreated control neutrophils (Fig. 4c) and colocalized with the azurophilic granule membrane protein CD63, indicative of delivery of NE via fusion of azurophilic granules with the phagosome. In addition, in contrast to untreated neutrophils, NE also translocated to the nucleus (Fig. 6d, asterisk) where it translocated away from CD63, associated with NE translocation during NETosis that is independent of membrane fusion events^{14, 15}. Therefore, the lower number of phagosomes formed per neutrophil upon dectin-1 inhibition, results in reduced NE sequestration, leaving enough NE to translocate to the nucleus and drive NETosis.

Furthermore, we observed a dramatic increase in NET induction in the lungs of dectin-1-deficient mice infected with the lung pathogen *A. fumigatus* (Fig. 6e) and WT *C. albicans* (Supplementary Fig. 6a) as compared to WT control mice. Staining of these lung sections with an antibody against the neutrophil specific marker MPO, suggested that the difference in NET formation was not due to lower numbers of neutrophils being recruited to the lung of WT mice (Fig. 6e). Our *in vitro* data suggested that aberrant NETosis in dectin-1-deficient mice was the result of deregulated suppression of NETosis in response to yeast. Indeed, *hgc1* yeast-locked *C. albicans* induced NET release in the lungs of dectin-1-deficient mice but failed to induce NETosis in WT mice (Fig. 7a). Moreover, there was no significant difference in the *hgc1* yeast-locked *C. albicans* burden in the lungs of dectin-1-deficient and WT mice, ruling out that differences in NETosis were due to higher fungal load (Supplementary Fig. 6b). Therefore, genetic disruption of phagocytosis in dectin-1-deficient animals leads to deregulation of NETosis and results in neutrophils releasing NETs in response to both yeast and hyphae.

Dectin-1 deficiency promotes NET-mediated pathology

Finally, we sought to address whether this mechanism for suppression of NETosis in response to small microbes like yeast is important in protecting against potential damage by excessive NET release. Aberrant NETosis is implicated in a range of inflammatory and autoimmune diseases^{37,38}. NETs are toxic to endothelial cells in culture³⁹⁻⁴¹, but the destructive role of NETs to tissues has not been addressed *in vivo*. We hypothesized that dysregulation of selective NETosis in dectin-1-deficient mice may lead to pathology. We infected WT and dectin-1-deficient mice with a high dose of *hgc1* yeast-locked *C. albicans* and assessed survival. We also treated these mice with either a specific NE inhibitor (NEi) that blocks NETosis¹⁴ or the tissue growth factor amphiregulin (AREG) that promotes tissue repair. Previous studies show that dectin-1-deficient mice exhibit impaired cytokine responses and are better protected against cytokine-induced shock^{42,43}. Dectin-1-mediated activation drives the upregulation of pro-inflammatory cytokines such as interleukin-6 (IL-6), IL-12 and tumor necrosis factor α (TNF) that can promote mortality during infection. Consistently, WT mice succumbed to infection with a high dose of *hgc1* yeast-locked *C. albicans* (Fig. 7b) and could not be rescued with NEi suggesting that NETs were not implicated in the pathology of WT mice. In addition, AREG treatment did not increase survival in WT mice (Fig. 7b), indicating that tissue damage was not influencing mortality. Instead, the lungs of WT mice exhibited substantially higher TNF concentrations than dectin-1-deficient lungs (Supplementary Fig. 6c) suggesting that WT mice succumb due to cytokine-induced shock.

Dectin-1-deficient mice also succumbed to the infection although their neutrophils are able to phagocytose yeast, albeit with lower capacity and can respond with significantly increased NETosis. Microbial load was comparable between the WT and dectin-1-deficient mice indicating that mortality of the mutant mice was not due to higher microbial load resulting from insufficient fungal clearance (Supplementary Fig. 6b). Instead, when NETosis was blocked with NEi (Fig. 7a) or when tissue repair was promoted with AREG treatment, infected dectin-1-deficient mice exhibited enhanced survival, suggesting that NETs were not only irrelevant in protecting these mice against the yeast-locked *C. albicans* strain, but were

detrimental to the host when present at high amounts (Fig. 7b). The yeast-locked *hgc1* mutant elicited substantial neutrophil infiltration in the lungs of both WT and dectin-1-deficient mice (Fig. 7a and Supplementary Fig. 6d), indicating that differences in survival were not due to changes in neutrophil recruitment but in subsequent neutrophil responses. The comparable fungal load in both groups of mice suggested that neutrophils were exposed to similar amounts of microbial stimuli during infection.

The effectiveness of the NEi and AREG treatments to rescue dectin-1 deficient mice suggested that their mortality was driven by aberrant NET release causing tissue damage. Indeed, in comparison to WT mice, the lungs of dectin-1-deficient mice exhibited increased tissue damage associated with fibrin deposition and substantial bleeding in response to *hgc1* yeast-locked *C. albicans* (Fig. 7c and Supplementary Fig. 7a). These symptoms were alleviated by treatment with NEi (Fig. 7c and Supplementary Fig. 7a), suggesting that NETs were driving tissue damage in the lungs of dectin-1-deficient animals. NE can also cause acute tissue damage directly⁴⁴⁻⁴⁶. In our analysis, NEi-treated WT mice exhibited a slight improvement in lung damage (Fig. 7c) and since NETs were absent in WT mice, some damage could have arisen through NET-independent mechanisms. However, because NETs form only in dectin-1-deficient, but not in WT mice, the inability of NEi to rescue WT mice indicates that the beneficial effect of the NEi and AREG in dectin-1-deficient animals was mediated through suppression of NET-driven damage and not NET-independent mechanisms. Otherwise, lung damage would have been comparable in WT and dectin-1-deficient mice. Therefore, while dectin-1 is important for potent cytokine induction, it is also critical in the regulation of neutrophil antimicrobial strategies (Supplementary Fig. 7b). By promoting phagocytosis of smaller microbes, this phagocytic receptor downregulates NETosis in a microbial size-dependent manner to minimize tissue damage during infection (Supplementary Fig. 7c).

DISCUSSION

Our findings identify a microbial size-sensing mechanism that allows neutrophils to selectively tailor their antimicrobial responses to pathogens based on microbial size. The decision that regulates NETosis relies on the competition of two cellular processes for NE. Phagocytosis is a rapid process, and neutrophils engulf a maximum number of yeast particles within 30-40 min. In contrast, NETosis is a slow process that takes approximately 4 h after encounter with hyphae. Phagocytosis drives the rapid fusion of azurophilic granules with the phagosome and the delivery of NE to its microbial contents to sequester NE away from the nucleus and prevent the proteolytic processing of histones that promotes chromatin decondensation during NETosis. When neutrophils encounter a microbe that is too large to be phagocytosed, the absence of phagosomes allows for NE to be slowly released into the cytosol via an alternative pathway that does not involve membrane fusion¹⁵. NE is then free to translocate to the nucleus and drive chromatin decondensation. This simple but effective mechanism allows phagocytes to distinguish between small and large pathogens. In contrast, the selective phagocytosis triggered by particle-associated cell wall components, such as β -glucan, over their soluble state is determined by the exclusion of suppressive phosphatase activity that triggers the phagocytosis cascade³. This mechanism does not seem to play a role in the discrepancy between smaller and larger particles, since, in contrast to soluble

ligands Syk, ERK and presumably other downstream kinases are sufficiently activated by both small yeast and large hyphae. Whether the mechanism we present here can serve as a paradigm for differences in cytokine release in response to these fungal forms in macrophages remains to be addressed.

Interestingly, neutrophils that have completed phagocytosis die with similar kinetics as neutrophils entering NETosis as indicated by the entry of the cell-impermeable Sytox dye. This suggests that neutrophils responding to yeast and hyphae enter a necrotic program that lyses the plasma membrane. However, chromatin remains condensed in response to yeast but decondenses in response to hyphae. These observations provide additional evidence to support a model where the two processes share the same upstream regulatory signaling pathway and the formation of phagosomes acts downstream to dictate the divergence of the NE signal towards phagocytosis or NETosis.

Moreover, during phagocytosis of smaller microbes and other particles, granules begin to fuse with the plasma membrane before membrane closure³². This results in some azurophilic granule contents leaking to the extracellular space during phagocytosis. Our immunofluorescence studies show that despite an engagement of neutrophils with hyphae that lasts for several hours before NET release, most of the NE remains inside the neutrophils and is not secreted. This suggests that azurophilic granules do not fuse significantly with the plasma membrane during this lengthy engagement.

Our findings define the criteria that determine whether a microbe will trigger NETosis. Small microbes that are taken up in a mature phagolysosome are not good stimuli for NETosis. This mechanism ensures that phagocytosis acts as a checkpoint that determines whether a neutrophil will deploy NETs. Here we demonstrate that microbial size is a critical factor that regulates NETosis in response to fungi and bacteria. Like large *C. albicans* hyphae, *M. bovis* BCG aggregates also triggered NETosis, while other single bacteria failed to induce the response. Our transwell experiments indicate that the upstream pathways that initiate NETosis are likely to be similar for most microbes and phagocytosis is the critical event that dictates the decision to form NETs. Furthermore, NETosis may provide an immune response to pathogenic bacteria that circumvent phagocytosis through virulence strategies that include the formation of large aggregates²⁶⁻²⁸ or the adoption of bacterial filamentous forms that delay phagocytosis⁴⁷. But microbial size may not be the only virulence mechanism that triggers NETosis. Some bacteria are phagocytosed but can prevent fusion of late endocytic organelles with the phagosome^{48, 49} or even rupture the phagosome⁵⁰. We propose that these virulence mechanisms may play a critical role in the induction of NETosis in response to bacterial stimuli. Notably, *M. tuberculosis* and *M. bovis* BCG are known to inhibit phagosome maturation. Our analysis suggests that in the case of *M. bovis* BCG, NETosis appeared to be dependent on microbial size, but one cannot exclude that bacterial-dependent manipulation of phagosome maturation may enhance NET release and further work is needed to address this. Macrophages also release extracellular traps (METs) in response to *M. tuberculosis*⁵¹ in a process that also depends on macrophage proteases, suggesting that neutrophil and macrophage extracellular traps may play important roles during infection. Interestingly, viruses like HIV trigger NET release⁵². Our model

predicts that viruses may be good NET stimuli since they may be too small to form substantially large endocytic organelles to significantly deplete NE³.

Importantly, the ability to release NETs selectively is critical to minimize unnecessary immune pathology associated aberrant NETosis^{19, 20}. Our data demonstrate that interference with phagocytosis through defects in dectin-1 disrupts the ability of neutrophils to make this important decision and release NETs indiscriminately, driving tissue damage and host mortality that can be rescued by pharmacological inhibition of NET formation. Interestingly, recent studies reported that low expression of dectin-1 and mutations in phagocytic receptors are associated with autoimmune pathologies^{53, 54}. Our findings suggest that these deficiencies may disrupt the regulation of selective NET release, triggering or exacerbating autoimmune disease symptoms.

Neutrophils have long been viewed as pathogenic effectors in a number of diseases. The mere presence of neutrophils at the inflammatory site signified pathology. Our findings contradict this simple model where neutrophils engage a variety of pathogens through a single antimicrobial program. Instead, after recruitment to the site of inflammation, neutrophils possess the capacity to make important decisions that define the antimicrobial strategies they will undertake in order to efficiently clear pathogens and minimize host damage.

ONLINE METHODS

Human peripheral neutrophils and NET release assay

Peripheral blood was collected from de-identified healthy adult volunteers according to the approved protocol of the NIMR Ethics board. Neutrophils were freshly isolated over Histopaque-/ Percoll- gradients as described elsewhere. 5×10^4 neutrophils per well were plated on the bottom of a 24-well plate in HBSS + Ca/Mg + 3 % human plasma. If not stated otherwise, neutrophils were stimulated with a MOI of 10 with *C. albicans* yeast or pre-formed hyphae. 4 h later Sytox (Invitrogen, S7020) was added and cells were analyzed for NET release. NET release was scored using ImageJ (NIH, Bethesda, MD, USA) as previously described¹⁴ and the results were plotted as the area of each Sytox positive event over total number of cells.

Fungal culture and hyphal preparation

WT (SC 5314) and yeast-locked (*hgc1*⁻) *Candida albicans* and WT *Aspergillus fumigatus* were cultured overnight in YEPD medium at 37°C. For all experiments *hgc1*⁻ yeast-locked *C. albicans* and *A. fumigatus* were subcultured in YEPD medium and WT *C. albicans* was subcultured in RPMI medium to induce hyphal growth for 4 h. Heat-inactivation was achieved by incubating *C. albicans* for 1 h at 90°C. Fragmentation of hyphae was carried out using the EmulsiFlex-C5 high-pressure homogenizer (Avestin).

Bacterial culture

E. coli and *K. pneumoniae* were cultured overnight in LB medium at 37°C and subcultured to an OD₆₀₀ of 1.

***M. bovis* BCG-dsRed preparation**

BCG-dsRed⁵⁵ was grown to an OD₆₀₀ of 0.8 in Middlebrook 7H9 medium supplemented with 10% Oleic acid, Albumin, Dextrose, Catalase (OADC), 0.05% Tween-80, 0.4% glycerol and 50ug/ml Hygromycin at 37°C with shaking at 100 rpm. Bacterial cultures were centrifuged and the supernatant was repeatedly passed through a syringe to remove large aggregates. The obtained single cells and small aggregates were used for experiments.

Transwell assay

The rims of conventional 24-well transwell plates (0.4 µm pore size, 10 µm membrane thickness) (Corning Incorporated) were cut off to enable the transwell strainer to sit directly on the bottom of the culture dish, allowing for direct contact with the neutrophils plated in the well. For stimulation, *C. albicans* yeast was seeded in the transwell strainer. 4h later neutrophils were analyzed for NET release as described above.

Confocal microscopy of fixed cells and tissue

5×10⁴ human peripheral neutrophils were plated on glass coverslips 1 h prior to stimulation. After stimulation, cells were fixed with 2% paraformaldehyde for 20 min at 37°C. Immunofluorescence staining was performed as described elsewhere. Anti-neutrophil elastase (NE) (Abcam), 4',6-Diamidino-2-phenylindole dihydrochloride (DAPI) (Life technologies), anti-human/mouse myeloperoxidase (MPO) (R&D Systems), anti-*C. albicans* (Acris), anti-p40 (Millipore, 1.22), anti-p47 (Santa Cruz), anti-CD63 (Millipore, RFAC4). For lung histology dissected lungs of infected mice were fixed over night in 2% paraformaldehyde and embedded in wax for sectioning. Sections were treated with a standard antigen retrieval protocol and immunofluorescence staining as described elsewhere. Cit-H3: anti-Histone H3 (citrulline R2 + R8 + R17) (Abcam, ab5103), MPO, DAPI. Stained cells and tissues were mounted and examined with confocal microscopy. Image analysis was performed using ImageJ.

Confocal microscopy of live cells and *M. bovis*

6×10⁵ human peripheral neutrophils were plated with Sytox on glass bottom petri dishes (MatTEK) and stimulated with a mixture of *M. bovis* single cells and aggregates. NET release was examined over a period of 4h. Time-lapse images were analyzed for NET release

Confocal microscopy of live cells and phagocytosis rate

3×10⁵ human peripheral neutrophils were plated on glass bottom petri dishes (MatTEK) and incubated for 1 h in the presence of anti-dectin-1 blocking antibody (AbD Serotec, BD6) prior to stimulation. Sytox was added for detection of NET release. Neutrophils were stimulated with *C. albicans* yeast or pre-formed hyphae and NET release was examined over a time of 4 h. Time-lapse images were analyzed for number of phagocytosed particles by recording the number of phagocytosed particles per cell for each frame.

Immunoblotting

1×10^6 human peripheral neutrophils were plated in 12-well plates. Neutrophils were stimulated with *C. albicans* yeast or pre-formed hyphae. At indicated times cells were lysed in SDS sample buffer and stored at -80°C . A standard immunoblotting protocol was carried out as described elsewhere. H3: anti-histone H3 (pan) (Millipore), Syk: anti-Syk (N-19) (Santa Cruz), pSyk: anti-phospho-Zap-70 (Tyr319)/Syk (Tyr352) (Cell Signaling), ERK: p44/42 MAPK (Erk1/2) (Cell Signaling), pERK: ERK1/2 (pTpY185/187) (Life Technologies).

Quantification of NE localization

Confocal z-series (every $0.8 \mu\text{m}$) covering the entire neutrophil were used to quantify total NE and NE co-localizing with the nucleus using ImageJ. For nuclear localization the NE signal was measured using a mask created with the corresponding DAPI (DNA) channel for each section. NE signals in individual sections were added to yield the total NE for each cell. 15-20 neutrophils per condition were processed.

Inhibition of vesicle fusion

5×10^4 neutrophils per well were plated on the bottom of a 24-well plate and pre-incubated for 1 h at 37°C in the presence of $1 \mu\text{M}$ bafilomycin (Sigma) or $2.5 \mu\text{M}$ nocodazole (Sigma). Subsequently neutrophils were stimulated with *hgc1* yeast-locked *C. albicans* (MOI = 10). NET release was assessed 4 h later as described above.

Phagocytosis of yeast or beads to inhibit NETosis

Small polystyrene beads ($3 \mu\text{m}$ diameter, Krisker biotech) were opsonized for 30 min at 37°C with 100% plasma prior to stimulation. 5×10^4 neutrophils per well were plated on the bottom of a 24-well plate and pre-incubated for 30 min at 37°C with *hgc1* yeast-locked *C. albicans* or polystyrene beads to induce phagocytosis. Afterwards neutrophils were stimulated with preformed *C. albicans* hyphae (MOI = 10). NET release was assessed 4 h later as described above.

Mouse infection and enumerating fungal load

All mouse experiments conformed to the guidelines of the UK home office under an approved project license. Mice were infected intratracheally with the indicated doses of *hgc1* yeast-locked or WT (pre-formed hyphae only where indicated) *C. albicans*. Weight and survival of mice were monitored daily. To assess fungal load, mouse organs (lungs and spleens) were dissected, homogenized in sterile saline and serial dilutions of the homogenates were spread onto sabourad dextrose agar plates. Colonies were counted after plate incubation at 37°C . NEi (GW611313A) (Sigma) and AREG (R&D Systems, 989-AR) were administered 4 h prior to infection and subsequently every 24 h.

Microbial strains

C. albicans WT clinical isolate SC 5314 and *hgc1* yeast-locked mutant²¹, *Aspergillus fumigatus* isolate 13073 (ATCC, Manassas, VA), *E. coli* DH5a, *K. pneumoniae* KP52145⁵⁶, *M. bovis* BCG-dsRed⁵⁵.

Supplementary Material

Refer to Web version on PubMed Central for supplementary material.

ACKNOWLEDGEMENTS

This work was supported by the Medical Research Council (UK) (MC_UP_1202/13 for VP and MC_UP_1202/11 for MGG) and the Wellcome Trust. We thank Yue Wang and Neil Gow for kindly providing the *hgc1* *C. albicans* strain, Gitta Stockinger, Marc Wilson and Arturo Zychlinsky for useful comments on the manuscript, Elliott Bernard for help with the *M. bovis* preparation and Adebambo Adekoya and Kathleen Mathers for support with animal experiments. All data necessary to understand this manuscript are presented in the main text or supplementary materials.

REFERENCES

1. Scianimanico S, et al. Impaired recruitment of the small GTPase rab7 correlates with the inhibition of phagosome maturation by *Leishmania donovani* promastigotes. *Cellular microbiology*. 1999; 1:19–32. [PubMed: 11207538]
2. Gantner BN, Simmons RM, Underhill DM. Dectin-1 mediates macrophage recognition of *Candida albicans* yeast but not filaments. *The EMBO journal*. 2005; 24:1277–1286. [PubMed: 15729357]
3. Goodridge HS, et al. Activation of the innate immune receptor Dectin-1 upon formation of a ‘phagocytic synapse’. *Nature*. 2011; 472:471–475. [PubMed: 21525931]
4. Gow NA, van de Veerdonk FL, Brown AJ, Netea MG. *Candida albicans* morphogenesis and host defence: discriminating invasion from colonization. *Nature reviews. Microbiology*. 2011; 10:112–122.
5. Joly S, et al. Cutting edge: *Candida albicans* hyphae formation triggers activation of the Nlrp3 inflammasome. *J Immunol*. 2009; 183:3578–3581. [PubMed: 19684085]
6. Arendrup MC. Epidemiology of invasive candidiasis. *Current opinion in critical care*. 2010; 16:445–452.
7. Low CY, Rotstein C. Emerging fungal infections in immunocompromised patients. *Fl000 medicine reports*. 2011; 3:14.
8. Urban CF, et al. Neutrophil extracellular traps contain calprotectin, a cytosolic protein complex involved in host defense against *Candida albicans*. *PLoS pathogens*. 2009; 5:e1000639. [PubMed: 19876394]
9. Borregaard N. Neutrophils, from Marrow to Microbes. *Immunity*. 2010; 33:657–670. [PubMed: 21094463]
10. Amulic B, Cazalet C, Hayes GL, Metzler KD, Zychlinsky A. Neutrophil function: from mechanisms to disease. *Annual review of immunology*. 2012; 30:459–489.
11. Brinkmann V, et al. Neutrophil extracellular traps kill bacteria. *Science*. 303:1532–1535. [PubMed: 15001782]
12. Metzler KD, et al. Myeloperoxidase is required for neutrophil extracellular trap formation: implications for innate immunity. *Blood*. 2011; 117:953–959.
13. Fuchs TA, et al. Novel cell death program leads to neutrophil extracellular traps. *The Journal of cell biology*. 2007; 176:231–241. [PubMed: 17210947]
14. Papayannopoulos V, Metzler KD, Hakkim A, Zychlinsky A. Neutrophil elastase and myeloperoxidase regulate the formation of neutrophil extracellular traps. *The Journal of cell biology*. 2010; 191:677–691. [PubMed: 20974816]
15. Metzler, Kathleen D.; Goosmann, C.; Lubojemska, A.; Zychlinsky, A.; Papayannopoulos, V. A Myeloperoxidase-Containing Complex Regulates Neutrophil Elastase Release and Actin Dynamics during NETosis. *Cell Reports*. 2014
16. Bianchi M, et al. Restoration of NET formation by gene therapy in CGD controls aspergillosis. *Blood*. 2009; 114:2619–2622. [PubMed: 19541821]

17. Lehrer RI, Cline MJ. Leukocyte myeloperoxidase deficiency and disseminated candidiasis - role of myeloperoxidase in resistance to *Candida* infection. *Journal of Clinical Investigation*. 1969; 48:1478–1488. [PubMed: 5796360]
18. Parry MF, et al. Myeloperoxidase deficiency - prevalence and clinical significance. *Annals of Internal Medicine*. 1981; 95:293–301. [PubMed: 6267975]
19. Branzk N, Papayannopoulos V. Molecular mechanisms regulating NETosis in infection and disease. *Semin Immunopathol*. 2013; 35:513–530. [PubMed: 23732507]
20. Caza T, Oaks Z, Perl A. Interplay of Infections, Autoimmunity, and Immunosuppression in Systemic Lupus Erythematosus. *International reviews of immunology*. 2014
21. Zheng X, Wang Y, Wang Y. Hgc1, a novel hypha-specific G1 cyclin-related protein regulates *Candida albicans* hyphal morphogenesis. *The EMBO journal*. 2004; 23:1845–1856. [PubMed: 15071502]
22. Martinez-Gomariz M, et al. Proteomic analysis of cytoplasmic and surface proteins from yeast cells, hyphae, and biofilms of *Candida albicans*. *Proteomics*. 2009; 9:2230–2252. [PubMed: 19322777]
23. Martchenko M, Alarco AM, Harcus D, Whiteway M. Superoxide dismutases in *Candida albicans*: transcriptional regulation and functional characterization of the hyphal-induced SOD5 gene. *Molecular biology of the cell*. 2004; 15:456–467. [PubMed: 14617819]
24. Grinberg N, Elazar S, Rosenshine I, Shpigel NY. Beta-hydroxybutyrate abrogates formation of bovine neutrophil extracellular traps and bactericidal activity against mammary pathogenic *Escherichia coli*. *Infection and immunity*. 2008; 76:2802–2807. [PubMed: 18411287]
25. Mori Y, et al. alpha-Enolase of *Streptococcus pneumoniae* induces formation of neutrophil extracellular traps. *The Journal of biological chemistry*. 2012; 287:10472–10481. [PubMed: 22262863]
26. Domenech M, Ramos-Sevillano E, Garcia E, Moscoso M, Yuste J. Biofilm formation avoids complement immunity and phagocytosis of *Streptococcus pneumoniae*. *Infection and immunity*. 2013; 81:2606–2615. [PubMed: 23649097]
27. Walker JN, et al. The *Staphylococcus aureus* ArlRS Two-Component System Is a Novel Regulator of Agglutination and Pathogenesis. *PLoS pathogens*. 2013; 9:e1003819. [PubMed: 24367264]
28. McAdow M, et al. Preventing *Staphylococcus aureus* sepsis through the inhibition of its agglutination in blood. *PLoS pathogens*. 2011; 7:e1002307. [PubMed: 22028651]
29. Bernut A, et al. *Mycobacterium abscessus* cording prevents phagocytosis and promotes abscess formation. *Proceedings of the National Academy of Sciences of the United States of America*. 2014; 111:E943–952. [PubMed: 24567393]
30. Hakkim A, et al. Activation of the Raf-MEK-ERK pathway is required for neutrophil extracellular trap formation. *Nature Chemical Biology*. 2011; 7:75–77. [PubMed: 21170021]
31. Drummond RA, Saijo S, Iwakura Y, Brown GD. The role of Syk/CARD9 coupled C-type lectins in antifungal immunity. *European journal of immunology*. 2011; 41:276–281. [PubMed: 21267996]
32. Nordenfelt P, Tapper H. Phagosome dynamics during phagocytosis by neutrophils. *J Leukoc Biol*. 2011; 90:271–284. [PubMed: 21504950]
33. Mollinedo F, et al. Combinatorial SNARE complexes modulate the secretion of cytoplasmic granules in human neutrophils. *J Immunol*. 2006; 177:2831–2841. [PubMed: 16920918]
34. Herre J, et al. Dectin-1 uses novel mechanisms for yeast phagocytosis in macrophages. *Blood*. 2004; 104:4038–4045. [PubMed: 15304394]
35. Kennedy AD, et al. Dectin-1 promotes fungicidal activity of human neutrophils. *European journal of immunology*. 2007; 37:467–478.
36. Watson RW, Redmond HP, Wang JH, Condrón C, Bouchier-Hayes D. Neutrophils undergo apoptosis following ingestion of *Escherichia coli*. *J Immunol*. 1996; 156:3986–3992. [PubMed: 8621940]
37. Garcia-Romo GS, et al. Netting neutrophils are major inducers of type I IFN production in pediatric systemic lupus erythematosus. *Science translational medicine*. 2011; 3:73ra20.
38. Kaplan MJ. Role of neutrophils in systemic autoimmune diseases. *Arthritis research and therapy*. 2013; 15:219. [PubMed: 24286137]

39. Villanueva E, et al. Netting neutrophils induce endothelial damage, infiltrate tissues, and expose immunostimulatory molecules in systemic lupus erythematosus. *J Immunol.* 2011; 187:538–552. [PubMed: 21613614]
40. Gupta AK, et al. Activated endothelial cells induce neutrophil extracellular traps and are susceptible to NETosis-mediated cell death. *FEBS Lett.* 2010; 584:3193–3197. [PubMed: 20541553]
41. Carmona-Rivera C, Zhao W, Yalavarthi S, Kaplan MJ. Neutrophil extracellular traps induce endothelial dysfunction in systemic lupus erythematosus through the activation of matrix metalloproteinase-2. *Annals of the rheumatic diseases.* 2014
42. Taylor PR, et al. Dectin-1 is required for beta-glucan recognition and control of fungal infection. *Nature immunology.* 2007; 8:31–38. [PubMed: 17159984]
43. Robinson MJ, et al. Dectin-2 is a Syk-coupled pattern recognition receptor crucial for Th17 responses to fungal infection. *The Journal of experimental medicine.* 2009; 206:2037–2051. [PubMed: 19703985]
44. Fujie K, et al. Release of neutrophil elastase and its role in tissue injury in acute inflammation: effect of the elastase inhibitor, FR134043. *Eur J Pharmacol.* 1999; 374:117–125. [PubMed: 10422648]
45. Ishii T, et al. Neutrophil elastase contributes to acute lung injury induced by bilateral nephrectomy. *The American journal of pathology.* 2010; 177:1665–1673. [PubMed: 20709801]
46. Kawabata K, Hagio T, Matsuoka S. The role of neutrophil elastase in acute lung injury. *Eur J Pharmacol.* 2002; 451:1–10. [PubMed: 12223222]
47. Prashar A, et al. Filamentous morphology of bacteria delays the timing of phagosome morphogenesis in macrophages. *The Journal of cell biology.* 2013; 203:1081–1097. [PubMed: 24368810]
48. Kusner DJ. Mechanisms of mycobacterial persistence in tuberculosis. *Clin Immunol.* 2005; 114:239–247. [PubMed: 15721834]
49. Deretic V. Autophagy, an immunologic magic bullet: Mycobacterium tuberculosis phagosome maturation block and how to bypass it. *Future microbiology.* 2008; 3:517–524. [PubMed: 18811236]
50. Simeone R, et al. Phagosomal rupture by Mycobacterium tuberculosis results in toxicity and host cell death. *PLoS pathogens.* 2012; 8:e1002507. [PubMed: 22319448]
51. Wong KW, Jacobs WR Jr. Mycobacterium tuberculosis Exploits Human Interferon gamma to Stimulate Macrophage Extracellular Trap Formation and Necrosis. *The Journal of infectious diseases.* 2013; 208:109–119. [PubMed: 23475311]
52. Saitoh T, et al. Neutrophil Extracellular Traps Mediate a Host Defense Response to Human Immunodeficiency Virus-1. *Cell host and microbe.* 2012; 12:109–116. [PubMed: 22817992]
53. Fossati-Jimack L, et al. Phagocytosis is the main CR3-mediated function affected by the lupus-associated variant of CD11b in human myeloid cells. *PloS one.* 2013; 8:e57082. [PubMed: 23451151]
54. Salazar-Aldrete C, et al. Expression and function of dectin-1 is defective in monocytes from patients with systemic lupus erythematosus and rheumatoid arthritis. *Journal of clinical immunology.* 2013; 33:368–377. [PubMed: 23097038]

REFERENCES FOR ONLINE METHODS

55. Kasmapour B, Gronow A, Bleck CK, Hong W, Gutierrez MG. Size-dependent mechanism of cargo sorting during lysosome-phagosome fusion is controlled by Rab34. *Proceedings of the National Academy of Sciences of the United States of America.* 2012; 109:20485–20490. [PubMed: 23197834]
56. Benghezal M, et al. Inhibitors of bacterial virulence identified in a surrogate host model. *Cellular microbiology.* 2007; 9:1336–1342. [PubMed: 17474906]

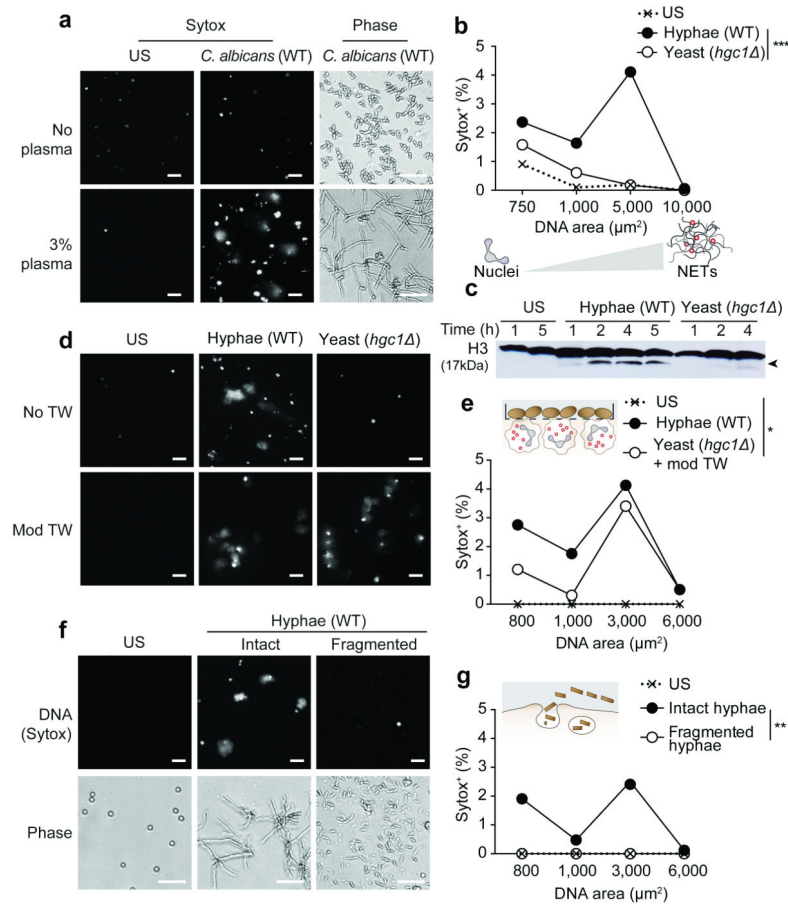


Figure 1. Hyphae selectively induce NETosis

(a) Human peripheral neutrophils stimulated with *C. albicans* with or without 3% plasma. Extracellular DNA stained for NET release with Sytox 4 h post stimulation. (b) Quantification of NET release by human peripheral neutrophils stimulated with a *hgc1* yeast-locked *C. albicans* mutant (yeast) or pre-formed WT *C. albicans* hyphae without plasma. Percentage (%) Sytox positive events over total number of neutrophils. (c) Histone H3 (17 kDa) degradation (arrow) of neutrophils stimulated with WT hyphae or *hgc1* yeast for the indicated times without plasma and assessed by immunoblotting. (d) NET release after direct stimulation of human peripheral neutrophils with *C. albicans hgc1* yeast or separated by a transwell that allows contact but prevents phagocytosis. (e) Quantification of (d). Percentage (%) Sytox positive events over total number of neutrophils. (f) NET release after stimulation of human peripheral neutrophils with intact or fragmented WT *C. albicans* hyphae. (g) Quantification of (f). % Sytox positive events over total number of neutrophils. (a-g) US, unstimulated. Multiplicity of infection (MOI) = 10. Scale bars = 50 µm. Statistics by one-way ANOVA, followed by Tukey's multiple comparison post test: * $p < 0.01$, ** $p < 0.001$, *** $p < 0.0001$. Data are representative of at least three independent experiments.

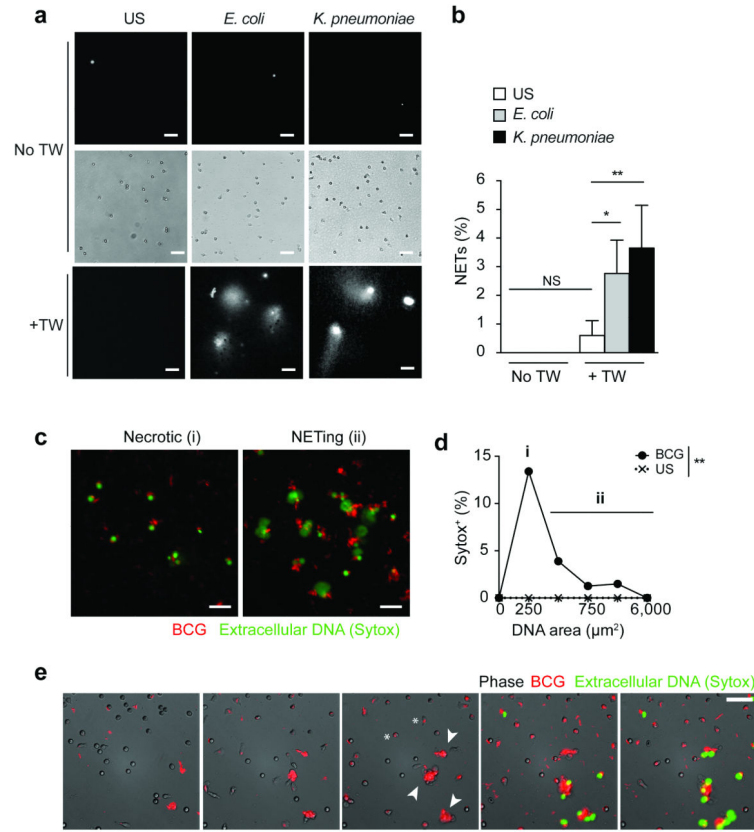


Figure 2. Single bacteria do not induce NET release

(a) NET release after direct stimulation of human peripheral neutrophils with *E. coli* DH5 α or *K. pneumoniae* KP52145 (MOI = 10) or separated by a transwell that allows contact but prevents phagocytosis. Extracellular DNA stained for NET release with Sytox 4 h post stimulation. US, unstimulated. Scale bars = 50 μm . (b) Quantification of (a). % NETs released over total number of neutrophils. Statistics by one-way ANOVA, followed by Sidak's multiple comparison post test: NS $p > 0.5$, * $p < 0.001$, ** $p < 0.0001$. Data are representative of three independent experiments. (c) NET release (Sytox, green) 4 h after stimulation of human peripheral neutrophils with BCG-dsRed. Scale bars: 50 μm . Necrotic neutrophils responding to single BCG and small aggregates (i) and NETting neutrophils responding to large BCG aggregates (ii). (d) Quantitation of NET release in (c) depicting the two neutrophil distributions (i, ii). Percentage (%) Sytox positive events over total number of neutrophils. Statistics by one-way ANOVA, followed by Tukey's multiple comparison post test: ** $p < 0.0001$. Data are representative of two independent experiments. (e) Time-lapse video microscopy stills of BCG-dsRed single bacteria (asterisks) and large aggregates (arrows) (red) incubated with human neutrophils in the presence of Sytox (green, extracellular DNA). Scale bar: 150 μm

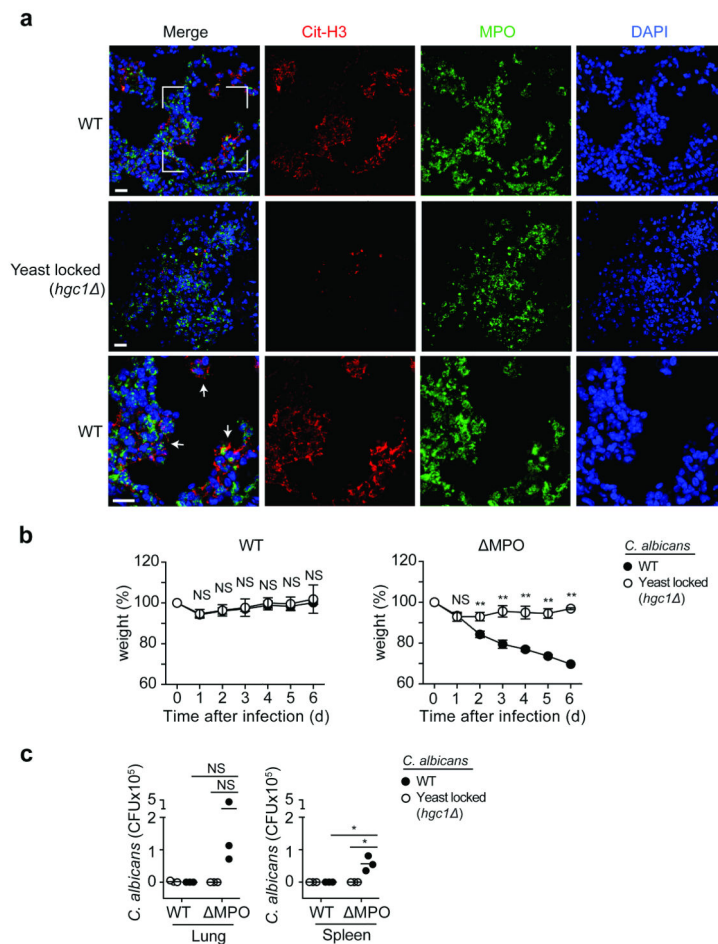


Figure 3. Selective NETosis is critical for clearance of hyphae *in vivo*

(a) NET release in the lungs of WT (C57BL/6) mice infected intratracheally with 1×10^5 c.f.u. WT *C. albicans* or a *hgc1* yeast-locked mutant and assessed 24 h post infection by immunofluorescence microscopy for citrullinated histone H3 (Cit-H3, red), MPO (green) and DNA (DAPI, blue). White arrows depict areas of NET release. Lower panel: magnification detail in upper panel. Scale bars = 20 μ m. (b) Weight of WT (C57BL/6) (n=6) and MPO deficient (n=5) mice infected with 1×10^4 c.f.u. WT *C. albicans* or a *hgc1* yeast-locked mutant. Weight normalized to starting weight at d0. Statistics by two-way ANOVA, followed by Sidak's multiple comparison post test: NS $p > 0.5$, ** $p < 0.0001$. (c) *C. albicans* load in the lung and spleen 6 days post infection (n=3). Statistics by two-way ANOVA, followed by Tukey's multiple comparison post test: NS $p > 0.5$, * $p < 0.01$. Data are representative of two independent experiments.

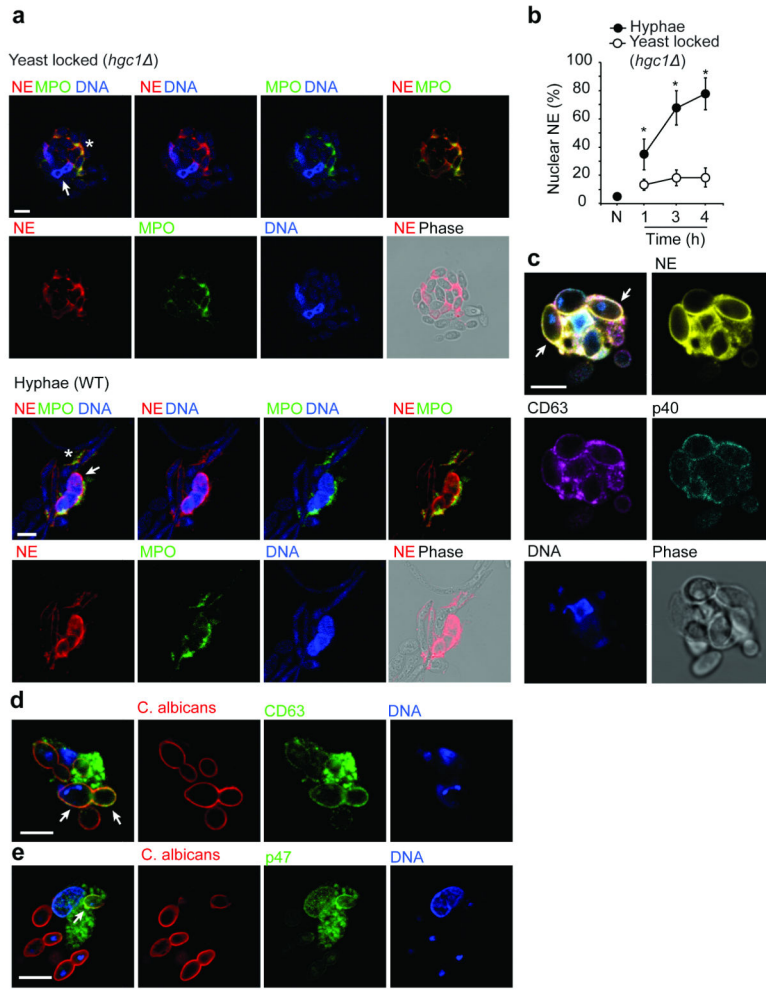


Figure 4. Only hyphae trigger NE translocation to the nucleus

(a) Human peripheral neutrophils stimulated with WT hyphae or *hgc1* yeast-locked mutant *C. albicans*. NE (red) and MPO (green) localization were assessed after 1 h by immunofluorescence via confocal microscopy. An optical section spanning the center of the cell is shown. Arrows indicate the nucleus. Asterisks indicate NE colocalisation with MPO. Scale bars = 5 μ m. Data are representative of two independent experiments. (b) Quantification of (a). Nuclear NE over total NE per cell from multiple confocal sections of 15-20 cells per condition. Statistics by two-way ANOVA, followed by Sidak's multiple comparison post test * $p < 0.0001$. (c) Human peripheral neutrophils stimulated with *hgc1* yeast-locked *C. albicans*. NE (yellow), CD63 (magenta), p40 (cyan) and DNA (DAPI, blue) localization after 1 h. Scale bar = 5 μ m. (d, e) Human peripheral neutrophils stimulated with *hgc1* yeast-locked *C. albicans* (red). CD63 (green) (d) or p47 (green) (e) and DNA (DAPI, blue) localization after 1 h. Scale bar = 5 μ m. Data are representative of three independent experiments (b–e).

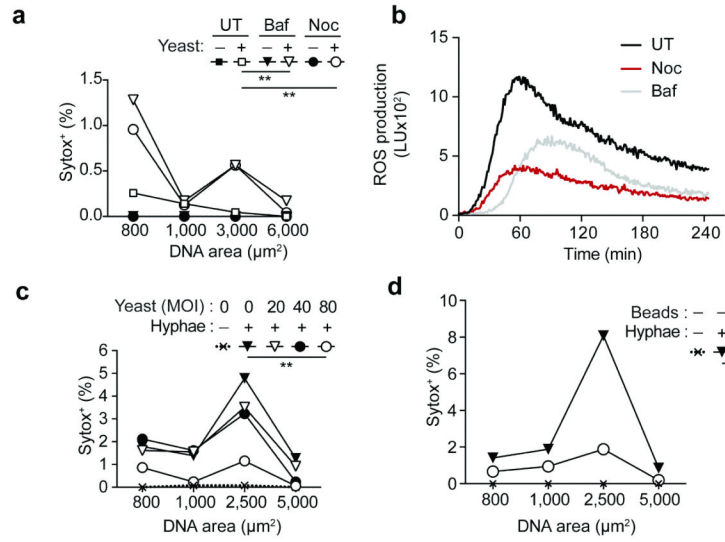


Figure 5. Phagocytosis inhibits NETosis by sequestration of NE

(a) NET release by human peripheral neutrophils untreated or treated with bafilomycin A1 (Baf, 1 μ M) or nocodazole (Noc, 2.5 μ M) and stimulated with *hgc1* yeast-locked *C. albicans* (MOI = 10). (b) Production of reactive oxygen species by human peripheral neutrophils untreated or treated with bafilomycin A1 (Baf) or nocodazole (Noc) and stimulated with *hgc1* yeast-locked *C. albicans* (MOI = 10). (c) NET release by neutrophils pre-incubated with *hgc1* yeast-locked *C. albicans* at an MOI of 0, 20, 40 and 80 for 1 h and stimulated with *C. albicans* hyphae at an MOI of 10. (d) NET release by neutrophils pre-incubated with 0.1 μ m polystyrene beads 1 h and stimulated with *C. albicans* hyphae at an MOI of 10. (a, c, d) Statistics by two-way ANOVA, followed by Sidak's multiple comparison post test: * $p < 0.01$, ** $p < 0.0001$. Data are representative of at least three independent experiments. UT, untreated; LU, luminescence units.

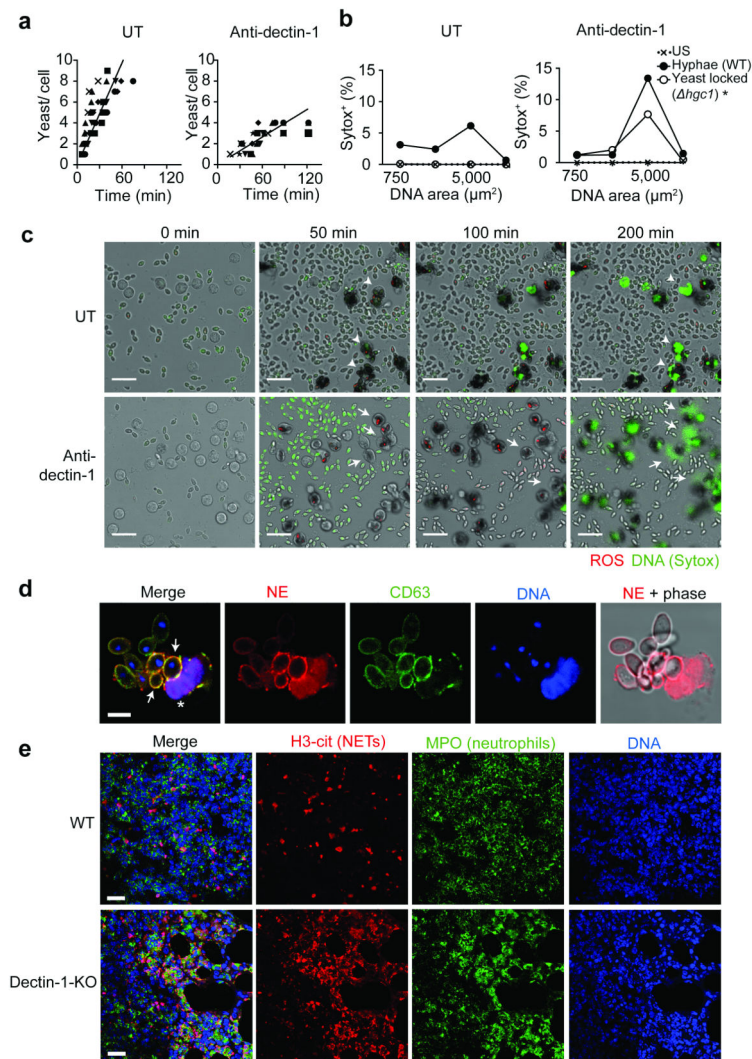


Figure 6. The phagocytic receptor dectin-1 negatively regulates NETosis

(a) Phagocytosis of *hgc1* yeast-locked *C. albicans* (MOI 40) by untreated neutrophils (left panel) or treated with anti-dectin-1 blocking antibody (right panel). The number of phagocytosed yeast particles per cell was assessed over 2 h by live microscopy. A trend line was fitted to the data from 10 individual neutrophils. (b) NET release by untreated peripheral human neutrophils (left panel) or treated with anti-dectin-1 blocking antibody (right panel) stimulated with *hgc1* yeast-locked *C. albicans* or WT hyphae (MOI = 10). Assessment of NET release 4 h post stimulation. % NETs released over total number of neutrophils. Statistics by one-way ANOVA, followed by Sidak's multiple comparison post test: * $p < 0.0001$ (c) Time-lapse microscopy of live human peripheral neutrophils treated with dectin-1 blocking antibody or left untreated and stimulated with heat-inactivated *hgc1* yeast-locked *C. albicans* (MOI = 40). Arrowheads indicate incomplete decondensation. Arrows indicate NET release. Confocal images were taken every 30 seconds. Panels represent frames of the indicated times. Scale bars = 20 μm . (d) Human peripheral neutrophils stimulated with *hgc1* yeast-locked *C. albicans*. NE (red), CD63 (green) and DNA (DAPI, blue) localization after 1 h. NE in the phagosome (arrows). NE in the nucleus

(asterisks). Scale bar = 5 μm . (e) NET release in the lungs of dectin-1 KO mice and WT (C57BL/6) controls infected intratracheally with 1×10^6 c.f.u. *A. fumigatus* assessed 48 h post infection by immunofluorescence staining against citrullinated histone H3 (H3-cit), MPO and DNA (DAPI). Scale bars = 20 μm . Data are representative of two independent experiments. UT, untreated. US, unstimulated.

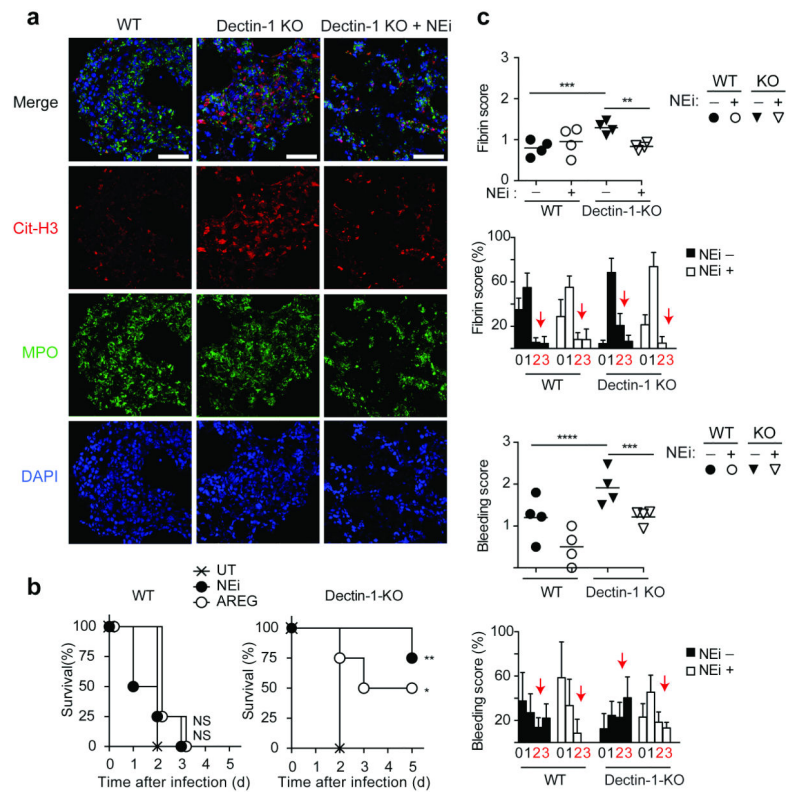


Figure 7. Deregulation of NET release leads to pathology

(a) Survival of WT (C57BL/6) and dectin-1 deficient mice, untreated or treated with NEi or AREG, infected intratracheally with 1×10^7 c.f.u. *hgc1* yeast-locked *C. albicans* ($n=4$). Statistics by Log-rank (Mantel-Cox) test, NS $p > 0.5$, * $p < 0.05$, ** $p < 0.01$. (b) NET release in lungs of WT (C57BL/6) and dectin-1-deficient mice treated with NEi prior to infection or left untreated, infected with 3×10^6 c.f.u. *hgc1* yeast-locked *C. albicans*. NET release 24 h post infection. Lungs sections stained for DNA (DAPI, blue), citrullinated histone H3 (cit-H3, red) and MPO (green) and analyzed by immunofluorescence confocal microscopy. Scale bars = 50 μ m. (c) Quantification of fibrin deposition (i, ii) and bleeding (iii, iv) in lungs of WT (C57BL/6) and dectin-1 deficient mice infected with of 3×10^6 c.f.u. *hgc1* yeast-locked *C. albicans*, assessed 36 h post infection with scores from 0 to 3. Average score for each mouse (i, iii) and percent of analyzed images from all mice that fall within each score (ii, iv). Fibrin score: 0 = none, 1 = >1 , 2 = $<50\%$, 3 = $<50\%$. Bleeding score: 0 = none, 1 = mild, 2 = moderate, 3 = severe. Statistics by two-way ANOVA, followed by Tukey's multiple comparison post test: ** $p < 0.01$, *** $p < 0.001$, **** $p < 0.0001$. Data are representative of two independent experiments.